Journal of Physical Sciences, Vol. 23, 2018, 171-188
ISSN: 2350-0352 (print), www.vidyasagar.ac.in/publication/journal
Published on 24 December 2018

Efficient Coupling of a Laser Diode to a Upside Down Tapered Microlens Tipped Circular Core Photonic Crystal Fiber using ABCD Matrix Formalism

Sumanta Mukhopadhyay

Department of Physics, St. Paul's Cathedral Mission College
33/1 Raja Rammohan Roy Sarani, Kolkata-700009, West Bengal, India
Email: sumukherjee_74@yahoo.com

Received 10 August 2018; accepted 30 November 2018

ABSTRACT

We investigate theoretically the coupling optics involving a laser diode and a series of circular core photonic crystal fibers with different air filling ratio and hole-pitch via upside down tapered microlens of two specific taper lengths on the tip of such fibers in absence of possible transverse and angular misalignments. By employing Gaussian field distributions for both the source and the fiber and also the already derived ABCD matrix for upside down tapered microlens, we formulate analytical expressions for the concerned coupling efficiencies for practically interesting two different light emitting wavelengths of 1.3 μm and 1.5 μm, respectively. Further, it is observed that, for a fit taper length of 70.0 μm of upside down tapered microlens, photonic crystal fiber with air filling ratio of 0.35 and hole-pitch of 5.0 μm comes out to be the most suitable one to couple laser diode emitting light of wavelength $\lambda = 1.3\mu m$. Moreover, the coupling efficiency can reach to 94.63% with simultaneous optimization of taper length and source position of specific lensed fiber. Such analysis which as per our knowledge is the first theoretical investigation, will be extremely important in ongoing investigations for the design of optimum launch optics involving upside down tapered microlens on the tip of photonic crystal fiber.

Keywords: ABCD matrix; Upside down tapered microlens; Circular core photonic crystal fiber; Optical coupling

1. Introduction

Photonic crystal fibers (PCFs), also known as microstructured optical fibers, have attracted a considerable amount of attention recently, because of their unique properties that are not realized in conventional optical fibers (COFs) [1]. Consequently, an efficient coupling between laser diodes (LDs) and single-mode fibers (SMFs) is one of the most basic, important technical aspects for constructing practical fiber transmission networks employing erbium-doped optical fiber amplifiers and it is always the hot investigative field in recent years. The design and fabrication of different integral microlenses on the tip of the SMF is the most popular scheme to improve the coupling efficiency. These microlenses, whether conical or hemispherical, possess the advantage of being self-centred. Due to ease of fabrication, hemispherical microlens on the tip of the SMF is very popular. The coupling optics involving hemispherical microlens on the tip of COF like circular core graded index single mode fiber (CCGISMF) have been recently studied [2]. On the other hand, because of high design flexibility of the PCFs compared to COFs, important optical properties can be tailored in PCFs [3]. These properties include endlessly single modeness, large mode area, high numerical aperture, high birefringence, high nonlinear coefficient, and tailorable large dispersion [3, 4]. The coupling optics involving hemispherical microlens on the tip of circular core photonic crystal fiber (CCPCF) [5] have produced relatively better results than that of CCGISMF [2]. In addition with hemispherical microlens, there are several other types of microlenses like hyperbolic, parabolic, elliptic, upside down tapered microlens which are popularly used for modulating the spot size of LD light incident on them and transmit it into the COF and PCF [2, 6-24]. Different methods have been proposed for optimization of coupling efficiency. For example, the variational formalism has been used in Ref. [25] to determine the fiber parameters and characteristics of graded index fibers using Marcuse spot sizes. However, the ABCD matrix technique has been widely used to analyze and design microlenses of different conic sections on the tip of the SMF. These ABCD matrix treatments are popular not only due to their simplicity but also for their predictability of such coupling efficiencies accurately with very little mathematical computations. It may be relevant to mention in this connection that the coupling optics involving hyperbolic microlens on the tip of the circular core step index single mode fiber (CCSISMF) [7, 8] as well as on the tip of CCGISMF [20] have been already reported based on previously formulated respective ABCD matrix [7, 8]. Moreover, the coupling optics involving hemispherical microlens on the tip of CCSISMF [9] as well as on the tip of CCGISMF [2] have also been already reported based on concerned theoretical ABCD matrix formalism [2, 9]. The coupling optics involving parabolic microlens on the tip of CCSISMF [15] as well as on the tip of CCGISMF [21] have been recently reported based on prescribed relevant ABCD matrix formalism [14].

Now, PCF is actually a unique type of pure silica optical fiber [1, 26, 27] with an array of air holes running along the entire length of the fiber, reminiscent of a crystal lattice, which gives to this type of fiber, its name. The central air hole of the structure has been omitted to form the core (Figure 1). Based on the light-guiding mechanism, PCFs can be classified into two main categories. The first one, air-guided hollow core PCFs in which light is guided by the photonic band-gap (PBG) effect, a mechanism that does not require a higher refractive index in the core to confine and guide light provided the frequency of the light is in the bandgap of two-dimensional photonic crystal formed by the periodic cladding. Different types of band gap PCFs such as all solid, low loss air core, have been also designed which find important applications that include gas sensing, CO_2 laser beam transmission, etc.[3].

On the other hand, the second one, index-guided solid core PCFs for which the lower effective refractive index of the surrounding holes forms the cladding and the light is confined to the central solid core as in COFs and guided by the process of modified total internal reflection (MTIR). The index-guiding fiber has a solid core region surrounded by a solid silica cladding, with periodically arranged air holes, whose effective refractive index depends on the ratio of air to glass, also known as the air filling ratio that comprises the structure. The presence of the holes in the cladding region reduces the effective refractive index of the cladding region, which will provide the variation of refractive index necessary to support total internal reflection at core cladding boundary. Therefore, the light is confined to the solid silica core, which has a relatively higher index than the effective cladding refractive index [3, 28, 29]. Moreover, PCFs can transport light with very low loss in certain wavelength where COFs possess very large loss [29]. Thus, in view of a wide range of favourable characteristics of PCFs, the study of this special kind of optical fiber is immensely necessitated.

The Gaussian approximation of the fundamental mode of non-circular core fiber like elliptic-core fiber has been detailed in Ref. [30] while the coupling optics involving LD and microlens on the tip of such elliptic core fiber have been detailed in Ref. [31]. However, the coupling efficiencies of hemispherical microlens as well as parabolic microlens are impaired due to limited aperture while fabrication of hyperbolic microlens is limited by involved technique**.** Recently upside down tapered microlens (UDTML) on the fiber tip, designed by tapering the fiber end into a large hemispherical shape, has also emerged [18, 32, 33] side by side as a new novel lensing scheme in coupling optics. UDTML may be utilized to accumulate a huge amount of light from the LD [32]. A detailed work on formation and power distribution properties of UDTML has been already reported in Ref. [32] while the corresponding structure of the UDTML fiber end and the refractive index distribution has already been highlighted in Ref. [33]. Thus, the study of coupling optics involving UDTML on the tip of SMF is of huge importance. Based on the prescribed transformation ABCD matrix of UDTML [18], the studies of the coupling losses in case of LD to CCSISMF [19] as well as on CCGISMF [22] coupling via UDTML on the tip of such fibers have also been already reported. It may be relevant to mention in this connection that the Fresnel backward reflection has been neglected to investigate the coupling efficiencies using UDTML on the tip of the CCSISMF [19] and CCGISMF [22].

Now, there are enormous amount of research works on microlenses like hyperbolic, hemispherical, parabolic, upside down tapered microlenses on the tip of different types of circular core COFs which have enriched the literature [2, 6-10, 14, 15, 17-22, 24, 32, 33] in the context of coupling optics. However, as per as research and developments related with microlensing coupling schemes on the tip of CCPCFs are concerned, different research papers investigating coupling of LD to solid core PCF via hyperbolic [11], hemispherical [5], parabolic [23] microlenses have been reported very recently using relevant ABCD matrix formalism. However, no such information is available regarding a study of coupling optics involving LD and CCPCF via UDTML on the tip of such fiber. Thus, our aim is to study the coupling losses in absence of possible transverse and angular misalignments in the case of a LD-to-CCPCF coupling via a UDTML on the tip of such fiber.

In the first part of this paper, we theoretically investigate the coupling efficiencies between a semiconductor LD emitting light of wavelength λ = 1.3 μm [10] and a series of typical CCPCFs with different air filling ratio d/Λ and lattice constant or hole-pitch Λ [5, 11, 23] via UDTML of two different taper lengths [19] on the tip of these fibers in absence of possible transverse and angular misalignments. In the second part, we carry out the similar investigation for a LD emitting light of wavelength λ =1.5 μm [10]. A comparison between these two cases is performed. As already stated, this analysis is based on previously derived simple ABCD matrix for refraction by a UDTML [18]. In fact, predictions of coupling optics by ABCD matrix method have produced excellent results as far as coupling of LD via UDTML of specific taper length on the tip of CCSISMF [19], and CCGISMF [22] are concerned. Concerned calculations need very little computations.

Further, we employ Gaussian field distributions for both the LD and the CCPCF. The present analysis, reported for the first time, contains significant new results in connection with the appropriate design of fiber geometry, i.e., core size, air hole pitch, the air hole size and the distribution of air holes, at a suitable wavelength emitted from the LD as well as that for the prediction of the suitable optogeometry of the UDTML. The results should be extremely important for the experimentalists, system designers and packagers who can, accordingly, mould and shape the desired UDTML at the CCPCF to achieve optimum coupling optics involving CCPCF in which air hole size, pitch, and distribution are additional degrees of freedom compared to COFs.

2. Analysis

2.1. Preview of UDTML structure and spot sizes of CCPCF

In this analysis, we consider the structure of the UDTML fiber end drawn from a SMF of core radius '*a*' as shown in Figure 1. Here, the radius of curvature R_0 and height '*h*' of the spherical end are related to the radius of aperture '$d^{/}$' by [18, 33]

$$R_0 = \frac{h^2 + d^{/2}}{2h} \tag{1}$$

where the radially symmetric axis OZ is actually the fiber axis and *r* and *z* represent the respective radial and axial coordinates, in the tapered region. The tapered surface equation is given by [18, 33]

$$r = d^{/}\left(1 - \frac{z}{L}\right) \tag{2}$$

where *L* is the length of the cone including the tapered region.

Now, in our present study, we consider an all-silica CCPCF having a triangular lattice of uniform structure for the air-hole and glass matrix elongated along the total length of the propagation direction of the fiber, as shown in Figure 1. The air-holes, each of diameter d, are distributed symmetrically around a central silica defect, which is actually an omitted air-hole, acting as the core of the said CCPCF. The infinite air-hole matrix with lattice-constant or hole-pitch Λ and air filling ratio d/Λ has been considered to act as the cladding of the CCPCF. Since the effective cladding index n_{FSM} is lesser than that of the core-index n_{CO}, the fiber can guide light by PBG mechanism for shorter wavelengths and by the mechanism of MTIR as in case of a conventional step index fiber (CSF) for longer wavelengths [5, 11, 12, 23].

Now, the fundamental modal field in a CCPCF is approximated as a Gaussian function [5, 11, 16, 23]

$$\psi_f = \exp\left[-\frac{x^2 + y^2}{w_{eff}^2}\right] \tag{3}$$

where w_{eff} corresponds to the spot size of the CCPCF.

The upper and lower limits of the propagation constants β of the guided modes through the core of the CCPCF satisfy [4, 5, 11, 12, 23]

$$k\, n_{CO} > \beta > \beta_{FSM} \tag{4}$$

where, $k=2\pi/\lambda$ being the wave number associated with the operating wavelength λ, n_{CO} is the refractive index of silica as the core material and β_{FSM} is the propagation constant of the fundamental space-filling mode (FSM), which is the fundamental mode in the infinite photonic crystal cladding without any defect or core.

The effective cladding index or the index corresponding to the FSM is [4, 5, 11, 12, 23]

$$n_{FSM} = \frac{\beta_{FSM}}{k} \tag{5}$$

The procedure for obtaining the value of n_{FSM} for given parameters of the CCPCF at operating wavelength of light has been detailed in Appendix A for ready reference [5, 11, 12, 23]. Here all the coefficients are determined by applying the least square fitting method for the operating wavelengths $\lambda = 1.3\mu m$ and $\lambda = 1.5\mu m$, presented in Tables 1 and 2, respectively. These coefficients have been utilized for determining the values of n_{FSM} of the CCPCF for various values of hole-pitch and the air filling ratio at any particular wavelength of interest [5, 11, 23].

$\lambda = 1.3\mu m$			
	$i=0$	$i=1$	$i=2$
A_i	1.430434	0.003803	-0.000214
B_i	0.069387	-0.012541	0.000650
C_i	-0.375746	0.107635	-0.008799

Table 1: Values of all coefficients required for the formulation of effective cladding index n_{FSM} at $\lambda = 1.3\mu m$.

$\lambda = 1.5\mu m$			
	$i=0$	$i=1$	$i=2$
A_i	1.432783	0.002170	-0.000036
B_i	0.063468	-0.007890	0.000147
C_i	-0.415418	0.114257	-0.009127

Table 2: Values of all coefficients required for the formulation of effective cladding index n_{FSM} at $\lambda = 1.5\mu m$.

The effective cladding index n_{FSM} can be utilized for finding the effective *V*-parameter of the CCPCF, treating the CCPCF like a CSF, with its cladding and core indices same as those of infinite photonic crystal structure and silica, respectively. Now the effective *V* value of the CCPCF is given by [5, 11-13, 23]

$$V_{eff} = \frac{2\pi}{\lambda} a_{eff} \left[n_{CO}^2 - n_{FSM}^2 \right]^{1/2} \tag{6}$$

where a_{eff} is the effective core radius which is assumed [5, 11-13, 23, 28] to be $\Lambda/\sqrt{3}$ and λ is the operating wavelength.

Then using Marcuse formula [16], the modal spot size w_{eff}, half of the mode field diameter (MFD) can be written as [5, 11, 12, 23]

$$\frac{w_{eff}}{a_{eff}} = 0.65 + \frac{1.619}{V_{eff}^{3/2}} + \frac{2.879}{V_{eff}^{6}} \tag{7}$$

The spot size of the CCPCF, w_{eff} is obtained by using Eq. (7), where V_{eff} being the effective *V*-parameter, calculated from Eq. (6). The method of such calculation has been detailed in Appendix A [5, 11, 12, 23].

2.2. Formulation of microlens coupling scheme

The coupling scheme to be studied has been presented in Figure 1. Here, '*u*' is the distance of separation between the LD and the UDTML end of the fiber. Again, in our analysis we use some usual approximations [2, 5-9, 11, 15, 19-23] like Gaussian field distributions for both the source and the fiber, perfect matching of the polarisation mode of the fiber field and that on the microlens surface, no transmission loss, sufficient angular width of the microlens to intercept the entire power radiated by the source for typical values of the microlens parameters employed. However, for the purpose of estimation of coupling optics using such LD and various kind of microlenses [2, 5, 7-9, 11, 15, 19-23], we simply use Gaussian beam with the elliptical waist spot sizes since the LDs we usually employ have dimensions of the parallel and perpendicular junctions fairly comparable [19].

The field Ψ_u representing the output of the LD at a distance *u* from the UDTML surface is taken as [19, 22, 30]

$$\Psi_u = \exp\left[-\left(\frac{x^2}{w_{1x}^2} + \frac{y^2}{w_{1y}^2} \right) \right] \exp\left[-\frac{ik_1}{2} . \frac{x^2 + y^2}{R_1} \right] \tag{8}$$

Here, w_{1x} and w_{1y} represent the spot sizes due to elliptical intensity profiles of the optical beams emitted from LD along two mutually perpendicular directions X and Y, one perpendicular and the other parallel to the junction planes, k_1 is the wave number in the incident medium and R_1 is the radius of curvature of the wavefronts from the LD. Our analysis is applicable to single frequency laser emitting only one spatial mode with a Gaussian intensity profile.

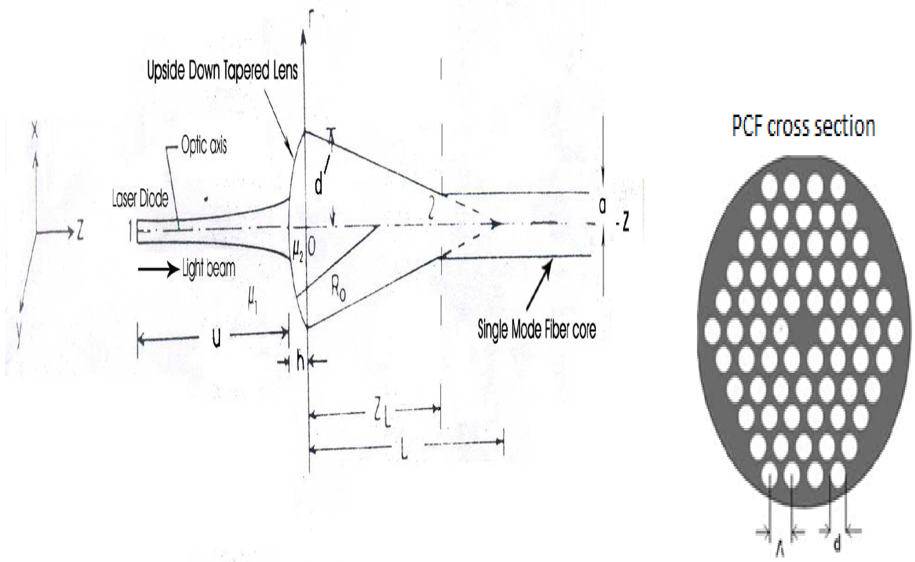

Figure 1: Geometry of LD to CCPCF coupling via UDTML on the fiber tip; μ_1 and μ_2 stand for refractive indices of incident and microlens media respectively.

The UDTML transformed laser field Ψ_v on the fiber plane 2 (plane for which z = z_L) as indicated in Figure 1 can be expressed as [19, 22, 30]

$$\Psi_v = \exp\left[-\left(\frac{x^2}{w_{2x}^2}+\frac{y^2}{w_{2y}^2}\right)\right]\exp\left[-\frac{ik_2}{2}\left(\frac{x^2}{R_{2x}}+\frac{y^2}{R_{2y}}\right)\right] \tag{9}$$

where w_{2x}, w_{2y} are respectively microlens transformed spot sizes and R_{2x}, R_{2y} being the respective transformed radii of curvature of the refracted wavefronts in the X and Y directions and k_2 being the wave number in the microlens medium. The method of finding w_{2x}, w_{2y}, R_{2x} and R_{2y} in terms of w_{1x}, w_{1y} and R_1 with the relevant ABCD matrix for UDTML [18, 19, 22] on the fiber tip is once again presented in the Appendix B for ready reference.

The source to fiber coupling efficiency via UDTML on the fiber tip is expressed in terms of well known overlap integral as mentioned below [2, 5, 7-9, 11, 15, 19-23, 31]

$$\eta = \frac{\left|\iint \Psi_v \Psi_f^* dxdy\right|^2}{\iint\left|\Psi_v\right|^2 dxdy \iint\left|\Psi_f\right|^2 dxdy} \tag{10}$$

Therefore η_0, the coupling efficiency in absence of misalignment, for CCPCF is given by [5, 11, 23]

$$\eta_0 = \frac{4w_{2x}w_{2y}w_{eff}^2}{\left[\left(w_{eff}^2 + w_{2x}^2\right)^2 + \frac{k_2^2 w_{2x}^4 w_{eff}^4}{4R_{2x}^2}\right]^{1/2}\left[\left(w_{2y}^2 + w_{eff}^2\right)^2 + \frac{k_2^2 w_{2y}^4 w_{eff}^4}{4R_{2y}^2}\right]^{1/2}} \quad (11)$$

However, Eq. (11) can be obtained by employing Eqs. (3) and (9) in Eq. (10).

3. Results and discussions

3.1. Optogeometrical parameters under consideration

Our formalism employs the relevant ABCD matrix under the paraxial approximation in order to predict the relevant coupling optics involving a LD and CCPCF via UDTML on the tip of the fiber. For the estimation of coupling efficiencies in absence of any possible transverse and angular misalignments for a UDTML of specific taper length on the tip of CCPCF, we firstly use a LD emitting light of wavelength $\lambda = 1.3\mu m$ with $w_{1x} = 1.081\mu m, w_{1y} = 1.161\mu m$ [10] and then LD emitting light of wavelength $\lambda = 1.5\mu m$ with $w_{1x} = 0.843\mu m, w_{1y} = 0.857\mu m$ [10]. The LD parameters used in this investigation are mentioned in Table 3. For the LD emitting light of abovementioned first wavelength, we study the coupling efficiencies for a series of typical CCPCFs having different air filling ratio d/Λ and hole-pitch Λ [5, 11, 23] as mentioned in Tables 4 and 5. Following [5, 11, 23], we choose three typical values of d/Λ, in the single moded region, ($d/\Lambda \le 0.45$) corresponding to two arbitrary Λ value (Λ = 4.5, 5.0 μm), as 0.35, 0.40, 0.45. Different calculated fiber spot sizes w_{eff} for these three d/Λ values corresponding to each Λ value (Λ = 4.5, 5.0 μm) are then utilized [5, 11, 12, 23] and shown in Tables 4 and 5 where we also present the relevant source positions with corresponding maximum coupling efficiencies for $\lambda = 1.3\mu m$.

LD	Wavelength λ in μm	Spot size w_{1x} in μm	Spot size w_{1y} in μm	λ_1 in μm	k_2 in μm^{-1}
#1	1.3	1.081	1.161	0.4138	7.4915
#2	1.5	0.843	0.857	0.4775	6.4926

Table 3: Laser diode parameters

Again as earlier, following [2, 5, 7-9, 11, 15, 19-23], the maximum depth of the microlens h is taken as $6.0\mu m$ while the refractive index $\mu(= \mu_2/\mu_1)$ of the material of the microlens with respect to surrounding medium is once again taken as 1.55. The core and cladding refractive indices are chosen as 1.46 and 1.45 respectively. The core diameter is taken as $2a$ = 4.0 μm. An UDTML to be drawn from those typical fibers is chosen with $2d'$ = 6.0 μm with UDTML length z_L as 23.3 μm and 26.6 μm corresponding to L being 70.0 μm and 80.0 μm, respectively. The radius of curvature R_0 of the spherical end of the UDTML is taken as 90.0 μm [19]. Further, as explained in earlier cases, since estimation of coupling efficiency on the basis of planar wave model differs insignificantly from that on the basis of spherical wave model [2, 5, 7-9, 11, 15, 19-23], we consider planar wave model for the input beam from the laser facet for the sake of simplicity.

Then we use a LD emitting light of wavelength $\lambda = 1.5\mu m$ with $w_{1x} = 0.843\mu m, w_{1y} = 0.857\mu m$ [10]. We compute again relevant source positions with resulting maximum coupling efficiencies for the above same set used in the first part of this investigation and present in Table 5.

3.2. Results for coupling scheme without misalignment consideration

From Tables 4 and 5, it is clear that the coupling efficiency can be improved through optimizing the working distance of the UDTML or in other words the source position is a key parameter that affects directly the coupling efficiency.

d/Λ	Λ (μm)	w_{eff} (μm)	L = 70.0 μm u(μm)	η_0	L = 80.0 μm u(μm)	η_0
0.35	4.5	3.957274	4.2	0.8933	1.9	0.9291
	5.0	4.433909	4.7	0.9463	2.2	0.9729
0.40	4.5	3.553313	3.5	0.8344	1.4	0.8734
	5.0	3.985642	4.2	0.8970	1.9	0.9323
0.45	4.5	3.236339	2.6	0.7812	0.8	0.8183
	5.0	3.627302	3.6	0.8460	1.5	0.8848

Table 4: Results for optimum coupling efficiency for a series of CCPCFs with different air filling ratio d/Λ and hole-pitch Λ via UDTML with different taper lengths L, at operating wavelength $\lambda = 1.3\mu m$. (u indicates source position, w_{eff} indicates fiber spot size and η_0 indicates coupling coefficient without misalignment)

$d^{/}$ = 3.0 μm, a = 2.0 μm, R_0 = 90.0 μm, h = 6.0 μm, μ = 1.55

Now from the results obtained in Table 4, it is observed that for a taper length L of 80.0 μm, the maximum coupling efficiency can reach to 97.29 % (i.e. coupling loss 0.1193 dB) when the source position u = 2.2 μm for the CCPCF with air filling ratio $d/\Lambda = 0.35$ and hole-pitch $\Lambda = 5.0\mu m$ having spot size w_{eff} of 4.433909 μm, in case of excitation by a LD emitting light of abovementioned first wavelength. On the other hand, it is observed that for a taper length L of 70.0 μm, the maximum coupling efficiency can reach to 94.63 % (i.e. coupling loss 0.2397 dB) when the source position u = 4.7 μm for the same CCPCF with air filling ratio $d/\Lambda = 0.35$ and hole-pitch $\Lambda = 5.0\mu m$ having spot size w_{eff} of 4.433909 μm.

d/Λ	Λ (μm)	w_{eff} (μm)	L = 70.0 μm u(μm)	η_0	L = 80.0 μm u(μm)	η_0
0.35	4.5	4.058139	3.9	0.6149	1.7	0.6640
	5.0	4.490145	4.4	0.6842	2.1	0.7370
0.40	4.5	3.625593	3.0	0.5437	1.1	0.5855
	5.0	4.026105	3.9	0.6096	1.7	0.6584
0.45	4.5	3.292278	2.0	0.4906	0.4	0.5234
	5.0	3.660019	3.1	0.5494	1.2	0.5919

Table 5: Results for optimum coupling efficiency for a series of CCPCFs with different air filling ratio d/Λ and hole-pitch Λ via UDTML with different taper lengths L, at operating wavelength $\lambda = 1.5\mu m$. (u indicates source position, w_{eff} indicates fiber spot size and η_0 indicates coupling coefficient without misalignment)

$d^{/}$ = 3.0 μm, a = 2.0 μm, R_0 = 90.0 μm, h = 6.0 μm, μ = 1.55

Moreover, from Table 5, it is once again observed that for the taper length L of 80.0 μm, the maximum coupling efficiency can reach to 73.70 % (i.e. coupling loss 1.3253 dB) when u = 2.1 μm for the CCPCF with $d/\Lambda = 0.35$ and $\Lambda = 5.0\mu m$ having spot size w_{eff} of 4.490145 μm, for excitation by a LD emitting light of abovementioned second wavelength. However, in case of taper length L of 70.0 μm, the maximum coupling efficiency can reach to 68.42% (i.e. coupling loss 1.6482 dB) when u = 4.4 μm for the CCPCF with $d/\Lambda = 0.35$ and $\Lambda = 5.0\mu m$ having spot size w_{eff} of 4.490145 μm, for excitation by a LD emitting light of abovementioned second wavelength.

It is seen from these Tables that for excitation by LDs emitting light of wavelengths $\lambda = 1.3\mu m$ and $\lambda = 1.5\mu m$, respectively, that the maximum coupling efficiency is achieved for the CCPCF with $d/\Lambda = 0.35$ and $\Lambda = 5.0\mu m$ with a UDTML of taper length L = 80.0 μm on its tip for excitation by LDs emitting light of the above mentioned two wavelengths. Moreover, the separation distances between the nearest point of the UDTML of a particular taper length and the LD have a very little difference comparatively in case of excitation by LDs emitting light of two wavelengths of practical interest. It is also observed that for a particular value of the air filling ratio d/Λ, the coupling efficiency increases with increase in hole-pitch Λ for excitation by a LD emitting a particular wavelength of light. On the other hand, it is prominent that for a particular value of the hole-pitch Λ, the coupling efficiency decreases with increase in air filling ratio d/Λ for excitation by a LD emitting a particular wavelength of light. However, the comparison between these results of coupling efficiencies for the CCPCF with $d/\Lambda = 0.35$ and $\Lambda = 5.0\mu m$ excited with two wavelengths predicts that the specific fiber with $d/\Lambda = 0.35$ and $\Lambda = 5.0\mu m$ are most suitable in the context of the aforesaid coupling optics involving CCPCFs and this excitement is uniquely excellent for a LD emitting specially light of wavelength $\lambda = 1.3\mu m$. Though the coupling efficiency for CCPCF with $d/\Lambda = 0.35$ and $\Lambda = 5.0\mu m$ excited with LD emitting light of wavelength $\lambda = 1.3\mu m$ are 94.63% and 97.29% respectively using UDTML with taper length 70.0 μm and 80.0 μm, but the source position for the first case is 4.7 μm while that for the second case is 2.2 μm. So far as the demand of achieving the merit of reasonable working distance to have maximum coupling efficiency on the tip of CCPCFs are concerned, this merit is acquired by CCPCF with $d/\Lambda = 0.35$ and $\Lambda = 5.0\mu m$ using UDTML with taper length 70.0 μm. However, the assembly of a LD in the close proximity of the UDTML within 4.7 μm is challenging to achieve in practice. But with the advent of new progress in nanotechnology, we are optimistic that the future technologist will involve any breakthrough to realize our result and test it experimentally. Moreover, these values of V_{eff} for light of wavelengths $\lambda = 1.3\mu m$ and $\lambda = 1.5\mu m$, respectively, correspond to low V region which is very well known for evanescent wave coupling in optical fiber directional coupler.

For a typical estimation of knowledge of excitation via UDTML with tapered length of 70.0 μm and 80.0 μm excited with LD #1 emitting light of wavelength $\lambda = 1.3\mu m$, respectively we present the variation of coupling efficiencies versus the source position for fibers corresponding to $d/\Lambda = 0.35$ and $\Lambda = 5.0\mu m$ and respective w_{eff} of 4.433909 μm, as shown in Figure 2. Figure 3 represents the same variation in case of excitation by LD # 2 emitting light of wavelength $\lambda = 1.5\mu m$. In these Figures, solid line (____ denoting EFF1) corresponds to L = 70.0 μm, dashed line (-------- denoting EFF2) to L = 80.0 μm. We see that although the values of the typical working distances relevant with the maximum coupling efficiencies corresponding to curves are not so much appreciable for excitation by a LD emitting a particular wavelength, the tolerance and also the optimum coupling efficiency, are relatively better observed when the corresponding most suitable CCPCF is excited with LD #1 emitting light of wavelength $\lambda = 1.3\mu m$.

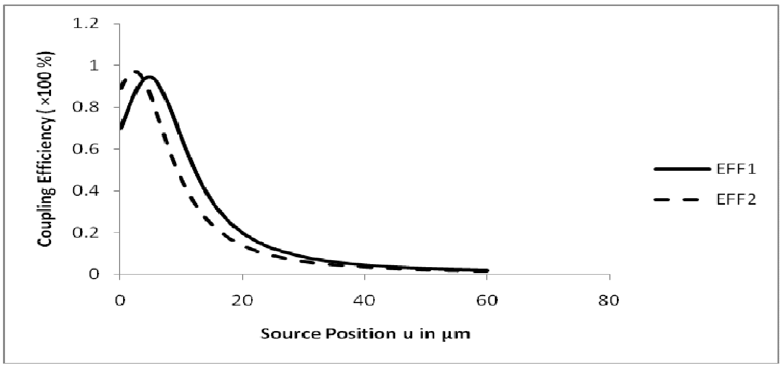

Figure 2: Variation of coupling efficiencies versus the source position for CCPCF having $d/\Lambda = 0.35$ and $\Lambda = 5.0\mu m$ and respective spot size w_{eff} of 4.433909 μm via UDTML with taper length of 70.0 μm and 80.0 μm, respectively excited with LD # 1 emitting light of wavelength $\lambda = 1.3\mu m$. Solid line (____ denoting EFF1) corresponds to L= 70.0 μm, dashed line (-------- denoting EFF2) to L= 80.0 μm.

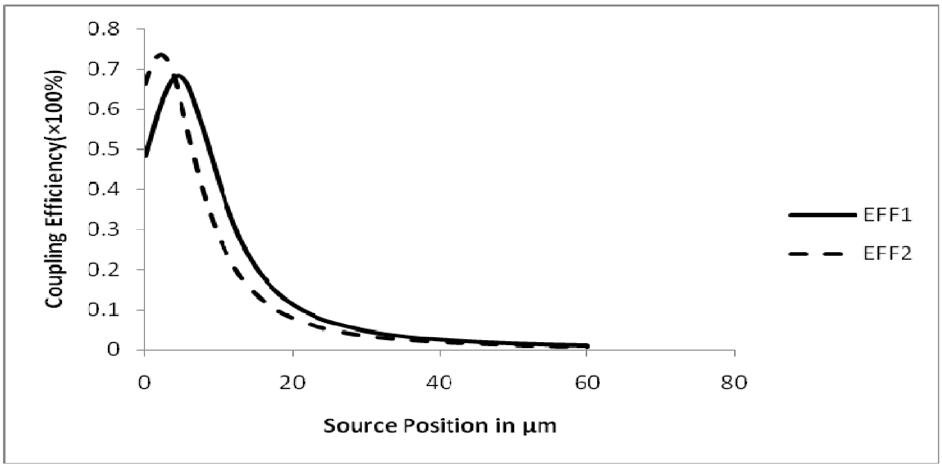

Figure 3: Variation of coupling efficiencies versus the source position for CCPCF having $d/\Lambda = 0.35$ and $\Lambda = 5.0\mu m$ and respective spot size w_{eff} of 4.490145 μm via UDTML with taper length of 70.0 μm and 80.0 μm, respectively excited with LD # 2 emitting light of wavelength $\lambda = 1.5\mu m$. Solid line (____ denoting EFF1) corresponds to L = 70.0 μm, dashed line (------- denoting EFF2) to L= 80.0 μm.

4. Conclusion

Employing ABCD matrix for refraction by a UDTML of two different taper lengths on the tip of a series of typical CCPCFs with different air filling ratio d/Λ and hole-pitch Λ, we present, for the first time, to the best of our knowledge, a simple but realistic method for evaluation of coupling efficiency for LD to CCPCF coupling in absence of possible transverse and angular mismatches. The best maximum coupling with optimization of appropriate source position is achieved for a CCPCF with air filling ratio of 0.35 and hole-pitch of 5.0 μm when excited with LD emitting light of wavelength $\lambda = 1.3\mu m$ using UDTML with taper length L = 70.0 μm. The optimized values of the taper length L= 70.0 μm of the UDTML are playing a crucial role in both cases. In comparison with the other deeply involved rigorous methods like Finite Difference Method and Finite Element Method, the application of novel ABCD matrix has simplified the analysis as the concerned calculations need very little mathematical calculations. Moreover, the method predicts acceptable air filling ratio and hole-pitch of the CCPCF from the point of view of fabrication of UDTML of allowable practical taper length. The technique developed should be useful in the system designing and packaging of suitable UDTML in coupling optics.

Appendix A:

The usual normalized parameters u and v for the infinite cladding region of the chosen CCPCF are given by [5, 11, 12, 23, 27]

$$u = k\Lambda\left(n_{CO}^2 - \frac{\beta^2}{k^2}\right)^{1/2} \qquad \text{(A1)}$$

and

$$v = k\Lambda\left(n_{CO}^2 - 1\right)^{1/2} \tag{A2}$$

with

$$u^2 + w^2 = v^2 . \tag{A3}$$

In order to obtain the effective cladding index n_{FSM} , a basic air-hole at the centre of a hexagonal unit cell is approximated to a circle in a regular photonic crystal [4, 5, 11, 12, 23]. Then from relevant boundary conditions for the fields and their derivatives in terms of appropriate special functions, corresponding to a fixed value of v, obtained from Eq. (A2) for fixed Λ and λ-values, the concerned u values are computed for different d ⁄ Λ values at a particular λ from the following equation, taking n_{CO} = 1.45 [5, 11, 23, 27]

$$\begin{aligned} &wI_1(a_n w)\left[J_1(bu)Y_0(a_n u) - J_0(a_n u)Y_1(bu)\right] \\ &+uI_0(a_n w)\left[J_1(bu)Y_1(a_n u) - J_1(a_n u)Y_1(bu)\right] = 0 \end{aligned} \tag{A4}$$

where $a_n = \dfrac{d}{2\Lambda}, \quad b = \left(\dfrac{\sqrt{3}}{2\pi}\right)^{1/2}$.

Using Eq. (A4), Russell has provided a polynomial fit to u, only for d/Λ = 0.4 and n_{CO} = 1.444. Further, for all d/Λ values of practical interest in the endlessly single mode region of a CCPCF, where d/Λ is less than 0.45, one should have a more general equation for wide applications [12].

The values of n_{FSM} are determined by replacing β/k in Eq. (A1) with n_{FSM} and this will lead to a modified simpler formulation of n_{FSM} as [5, 11, 12, 23]

$$n_{FSM} = A + B\left(\frac{d}{\Lambda}\right) + C\left(\frac{d}{\Lambda}\right)^2 \tag{A5}$$

where A, B and C are the three different optimization parameters, dependent on both the relative hole-diameter or hole-size d/Λ and the hole-pitch Λ.

Since optical communication window corresponds with two operating wavelengths of 1.3 μm and 1.5 μm, this study finds the coefficients for these two wavelengths of practical interest for different possible hole-sizes and hole-pitches of the CCPCF. Such modification in such a fitting is advantageous in the sense that it will help for reducing the computation time since only nine coefficients are required in calculation instead of twenty seven coefficients [5, 11, 12, 23].

Now, for each value of Λ with the variations of d/Λ, the n_{FSM} values corresponding to respective u values obtained from Eq. (A4) are determined. Applying least square fitting of n_{FSM} in terms of d/Λ to Eq. (A5) for a particular Λ, the values of A, B and C can be then estimated. The various values of A, B and C are then simulated for different Λ in the endlessly single mode region of the CCPCF, resulting in the empirical relations of A, B and C in Eq. (A5), in terms of Λ, as given in the following [5, 11, 12, 23]

$$A = A_0 + A_1\Lambda + A_2\Lambda^2 \quad \text{(A6)}$$

$$B = B_0 + B_1\Lambda + B_2\Lambda^2 \quad \text{(A7)}$$

$$C = C_0 + C_1\Lambda + C_2\Lambda^2 \quad \text{(A8)}$$

where A_i, B_i and C_i ($i = 0, 1$ and 2) are the optimization parameters for A, B and C, respectively. Computing A, B and C from Eqs. (A6-A8), one can find n_{FSM} directly for any d/Λ and Λ value at any particular λ using Eq. (A5) in the endlessly single mode region of the CCPCFs.

Appendix B:

Considering the distance *u* of the LD from the UDTML end, *q* parameters of the Gaussian beams at the input laser facet and the output microlens fiber interface can be related by the ABCD matrix as follows:

The input and output parameters (q_1,q_2) of the light beam is related by [19, 22]

$$q_2 = \frac{Aq_1 + Au + B}{Cq_1 + Cu + D} \quad \text{(B1)}$$

where

$$\frac{1}{q_{1,2}} = \frac{1}{R_{1,2}} - \frac{i\lambda_0}{\pi w_{1,2}^2 \mu_{1,2}} \quad \text{(B2)}$$

The ray matrix *M* for the UDTML on the fiber tip is given by [18, 19, 22]

$$M = \begin{pmatrix} A & B \\ C & D \end{pmatrix} \quad \text{(B3)}$$

where

$$A = r_2(z) - \frac{(1-\mu)r_1(z)}{\mu R_0} \quad \text{(B4a)}$$

$$B = \frac{r_1(z)}{\mu} \quad \text{(B4b)}$$

$$C = -\frac{(1-\mu)}{\mu R_0}\frac{dr_1(z)}{dz} + \frac{dr_2(z)}{dz} \quad \text{(B4c)}$$

$$D = \frac{1}{\mu}\frac{dr_1(z)}{dz} \quad \text{(B4d)}$$

The refractive index of the material of the microlens with respect to the incident medium is represented by $\mu(= \mu_2/\mu_1)$.

The *z* dependence of the above matrix elements can be explicitly expressed by substituting [18, 19, 22]

$$r_1(z) = -\frac{L}{\alpha}\left(1 - \frac{z}{L}\right)^{1/2} \sin k(z) \quad \text{(B5a)}$$

$$\frac{dr_1(z)}{dz} = \frac{1}{\left(1-\frac{z}{L}\right)^{1/2}}\left\{\cos k(z) + \frac{1}{2\alpha}\sin k(z)\right\} \quad \text{(B5b)}$$

$$r_2(z) = \left(1-\frac{z}{L}\right)^{1/2}\left\{\cos k(z) - \frac{1}{2\alpha}\sin k(z)\right\} \quad \text{(B5c)}$$

$$\frac{dr_2(z)}{dz} = \frac{A_0^2 L}{\left(1-\frac{z}{L}\right)^{1/2}\alpha}\sin k(z) \quad \text{(B5d)}$$

where

$$k(z) = \alpha \ln\left(1-\frac{z}{L}\right) \quad \text{(B6a)}$$

and $\alpha = \left(A_0^2 L^2 - 1/4\right)^{1/2}$ (B6b)

L being the tapered length or length of the cone including tapered region and A_0 is a constant given by

$$A_0 = \frac{1}{d^{/}}\left(2\ln\frac{n_{core}}{n_{clad}}\right)^{1/2} \quad \text{(B7)}$$

For a UDTML having aperture $2\,d^{/}$

$$z_L = \frac{L\left(d^{/} - a\right)}{d^{/}} \quad \text{(B8)}$$

In order to obtain $w_{2x,2y}$, the matrix is evaluated for $z = z_L$.

The transformed beam spot sizes and radii of curvature in the X and Y directions are found by using Eqs. (B4a-B4d) in Eqs. (B1) and (B2) and are given by

$$w_{2x,2y}^2 = \frac{A_1^2 w_{1x,1y}^2 + \frac{\left(\lambda_1^2 B_1^{\,2}\right)}{\pi^2 w_{1x,1y}^2}}{\mu(A_1 D_1 - B_1 C_1)} \quad \text{(B9)}$$

$$\frac{1}{R_{2x,2y}} = \frac{A_1 C_1 w_{1x,1y}^2 + \frac{\left(\lambda_1^2 B_1 D_1\right)}{\pi^2 w_{1x,1y}^2}}{A_1^2 w_{1x,1y}^2 + \frac{\left(\lambda_1^2 B_1^{\,2}\right)}{\pi^2 w_{1x,1y}^2}} \quad \text{(B10)}$$

where

$$\lambda_1 = \frac{\lambda_0}{\mu_1} \quad \text{(B11)}$$

$$A_1 = A + \frac{B_1}{R_1} \quad \text{(B12a)}$$

$$B_1 = Au + B \quad \text{(B12b)}$$

$$C_1 = C + \frac{D_1}{R_1} \quad \text{(B12c)}$$

$$D_1 = Cu + D. \quad \text{(B12d)}$$

In plane wavefront model, the radius of curvature R_1 of the wavefront from the laser facet $\rightarrow\infty$. This leads to A_1=A and C_1=C.

REFERENCES

1. A.Bjarklev, J.Broeng and A.S.Bjarklev, Photonic Crystal Fibres, Springer Science & Business Media Inc., NewYork, 2003.
2. A.Bose, S.Gangopadhyay and S.C.Saha, Laser diode to single mode circular core graded index fiber excitation via hemispherical microlens on the fiber tip: Identification of suitable refractive index profile for maximum efficiency with consideration for allowable aperture, Journal of Optical Communications, 33(1) (2012) 15-19.
3. R.Bhattacharya and S.Konar, Extremely large birefringence and shifting of zero dispersion wavelength of photonic crystal fibers, Optics & Laser Technology, 44 (2012) 2210–2216.
4. T.A.Birks, J.C.Knight and P.St.J.Russell, Endlessly single-mode photonic crystal fiber, Optics Letters, 22(13) (1997) 961-963.
5. S.Chakraborty, D.Roy, S.Mukhopadhyay and S.N.Sarkar, An Investigative Study of Efficient Coupling Mechanism of a Hemispherical Microlens Tipped Single Mode Photonic Crystal Fiber to a Laser Diode by ABCD Matrix Formulation and Determination of the Optimal Separation Distance, Optik, 149 (2017) 81–89.
6. C.A.Edwards, H.M.Presby and C.Dragone, Ideal microlenses for laser to fiber coupling, Journal of Lightwave Technology, 11 (1993) 252-257.
7. S.Gangopadhyay and S.N.Sarkar, Laser diode to single-mode fibre excitation via hyperbolic lens on the fibre tip: Formulation of ABCD matrix and efficiency computation, Optics Commuications, 132 (1996) 55-60.
8. S.Gangopadhyay and S.N.Sarkar, ABCD matrix for reflection and refraction of Gaussian light beams at surfaces of hyperboloid of revolution and efficiency computation for laser diode to single-mode fiber coupling by way of a hyperbolic lens on the fiber tip, Applied Optics, 36 (1997) 8582-8586.
9. S.Gangopadhyay and S.N.Sarkar, Laser diode to single-mode fiber excitation via hemispherical lens on the fiber tip: Efficiency computation by ABCD matrix with consideration for allowable aperture, Journal of Optical Communications, 19 (1998) 42-44.
10. J.John, T.S.M.Maclean, H.Ghafouri-Shiraz and J.Niblett, Matching of single- mode fibre to laser diode by microlenses at 1.5 μm wavelength, IEE Proceedings-Optoelectronics, 141 (1994) 178-184.
11. A.Karak, D.Kundu, S.Mukhopadhyay and S.N.Sarkar, Investigation of coupling of a laser diode to photonic crystal fiber via hyperbolic microlens on the fiber tip by ABCD matrix formalism, Optical Engineering, 54(8) (2015) 086102(1-7).
12. D.Kundu and S.Sarkar, Prediction of propagation characteristics of photonic crystal fibers by a simpler, more complete and versatile formulation of their effective cladding indices, Optical Engineering, 53(5) (2014) 056111(1-6).

13. M.Koshiba and K.Saitoh, Applicability of classical optical fiber theories to holey fibers, Optics Letters, 29(15) (2004) 1739–1741.
14. H.Liu, L.Liu, R.Xu and Z.Luan, ABCD matrix for reflection and refraction of Gaussian beams at the surface of a parabola of revolution, Applied Optics, 44 (2005) 4809-4813.
15. H.Liu, The approximate ABCD matrix for a parabolic lens of revolution and its application in calculating the coupling efficiency, Optik, 119 (2008) 666-670.
16. D.Marcuse, Loss analysis of single-mode fiber splices, The Bell System Technical Journal, 56(5) (1977) 703–718.
17. G.A.Massey and A.E.Siegman, Reflection and refraction of Gaussian light beams at tilted ellipsoidal surfaces, Applied Optics, 8 (1969) 975-978.
18. S.K.Mondal, S.Gangopadhyay and S.N.Sarkar, Analysis of an upside-down taper lens end from a single-mode step index fiber, Applied Optics, 37 (1998) 1006-1009.
19. S.K.Mondal and S.N.Sarkar, Coupling of a laser diode to single-mode fiber with an upside-down tapered lens end, Applied Optics, 38 (1999) 6272-6277.
20. S.Mukhopadhyay and S.N.Sarkar, Coupling of a laser diode to single mode circular core graded index fiber via hyperbolic microlens on the fiber tip and identification of the suitable refractive index profile with consideration for possible misalignments, Optical Engineering, 50(4) (2011) 045004(1-9).
21. S.Mukhopadhyay, Coupling of a laser diode to single mode circular core graded index fiber via parabolic microlens on the fiber tip and identification of the suitable refractive index profile with consideration for possible misalignments, Journal of Optics, 45(4) (2016) 312–323.
22. S.Mukhopadhyay, Laser Diode to Circular Core Graded Index Single Mode Fiber Excitation via Upside Down Tapered Microlens on the Fiber Tip and Identification of the Suitable Refractive Index Profile, Journal of Physical Sciences, 20 (2015) 173-187.
23. S.Mukhopadhyay, Efficient Coupling of a Laser Diode to a Parabolic Microlens Tipped Circular Core Photonic Crystal Fiber using ABCD Matrix Formalism with Consideration for Possible Misalignments, Journal of Optics, 47(1) (2018) 47–60.
24. H.M.Presby and C.A.Edwards, Near 100% efficient fibre microlenses, Electronics Letters, 28 (1992) 582-584.
25. P.Roy Chowdhury, A.Karak and S.Pramanik, Simple approach to find out fiber parameters and characteristics using Marcuse spot sizes applied to Variational Formalism, Journal of Physical Sciences, 18 (2014) 30-33.
26. P.St.J.Russell, Photonic crystal fibers, Science, 299(5605) (2003) 358-362.
27. P.St.J.Russell, Photonic-crystal fibers, Journal of Lightwave Technology, 24(12) (2006) 4729–4749.
28. K.Saitoh and M.Koshiba, Empirical relations for simple design of photonic crystal fibers, Optics Express, 13(1) (2005) 267-274.
29. M.Sharma, N.Borogohain and S.Konar, Index Guiding Photonic Crystal Fibers With Large Birefringence and Walk-Off, Journal of Lightwave Technology, 31 (2013) 3339-3344.
30. S.Sarkar, K.Thyagarajan and A.Kumar, Gaussian approximation of the fundamental mode in single-mode elliptic core fibers, Optics Communications, 49 (1984) 178-183.

31. S.N.Sarkar, B.P.Pal and K.Thyagarajan, Lens coupling of laser diodes to monomode elliptic core fibers, Journal of Optical Communications, 7 (1986) 92-96.
32. L.B.Yuan and R.L.Shou, Formation and Power Distribution Properties of an Upside Down taper Lens at the End of an Optical Fiber, Sensors and Actuators, A21-A23 (1990) 1158-1161.
33. L.Yuan and A.Qui, Analysis of a single-mode fiber with taper lens end, Journal of the Optical Society of America A, 9 (1992) 950-952.